# Target ionization and projectile charge changing in 0.5–8-MeV/$q$ $Li^{q+}$+He ($q$=1,2,3) collisions

O. Woitke,* P. A. Závodszky,† S. M. Ferguson, J. H. Houck, and J. A. Tanis
*Department of Physics, Western Michigan University, Kalamazoo, Michigan 49008*
(Received 14 July 1997; revised manuscript received 17 November 1997)

Target ionization and projectile charge changing were investigated for 0.5–8-MeV/$q$ $Li^{q+}$+He ($q$=1,2,3) collisions. Cross sections for the single and double ionization of He associated with no projectile charge change (direct ionization), single-electron capture, and single-electron loss were measured using coincidence techniques and compared to existing experimental and theoretical results. Total cross sections for single-electron capture (for $Li^{1,2,3+}$) and single-electron loss (for $Li^{1,2+}$) were also obtained. For a given incoming projectile charge state the double-to-single target ionization ratios $R$ vary strongly with the outgoing reaction channel. For direct ionization, $R$ is nearly independent of the incident projectile charge state and can be described by the semi-empirical scaling rule of Knudsen *et al.* [J. Phys. B **17**, 3545 (1984)]. However, for ionization associated with single-electron loss and single-electron capture by the projectile, $R$ depends quite strongly on the incident charge state of the projectile. These ionization ratios $R$ are interpreted in terms of theoretical formulations involving electron-nucleus interactions and electron-electron interactions. [S1050-2947(98)07704-X]

PACS number(s): 34.50.Fa, 34.70.+e

## I. INTRODUCTION

In this work, processes involving target ionization and projectile charge changing in ≈1 MeV/nucleon $Li^{1,2,3+}$+He collisions are investigated. These results are important in both fundamental and applied physics. For example, such studies can help test theories of few-body problems arising in atomic physics, specifically the interactions of nuclei with atomic electrons, and the interactions of electrons with other electrons [1]. For this purpose, the collision system $Li^{q+}$+He ($q$=1,2,3) is well suited because electron-electron effects can be observed both for the projectile and target. Helium is the simplest neutral target that shows electron-electron effects, while lithium can serve (a) as a fully stripped projectile, (b) a one-electron projectile, or (c) a two-electron projectile. In the latter case, the Li projectile can exhibit electron-electron effects itself. In this work target ionization associated with specific outgoing projectile charge states is investigated. While the target undergoes ionization, the projectile charge state can remain unchanged (direct ionization), it can capture an electron, or it can lose an electron.

Of particular interest is the double ionization of the He target associated with each of the above-mentioned projectile reaction channels. For the energy range investigated here, double ionization is examined in terms of mechanisms involving electron-nucleus (independent-particle) interactions as well as electron-electron (correlation) effects [1,2]. Double ionization by independent-particle interactions can be understood as two separate interactions (in the same collision event) of the projectile nucleus with each of the target electrons; this picture is valid for intermediate velocities (for which there is sufficient time for two interactions) such that $Z/v \gtrsim 0.2$ ($Z$ is the projectile atomic number and $v$ is the velocity in atomic units). For this case, Knudsen *et al.* [3] found empirically that $R \propto (Z/v)^2 \ln(v)^{-1}$. For velocities and charges such that $Z/v \lesssim 0.1$ [1,2], the probability of double ionization by two separate projectile-nucleus–target-electron interactions in a single collision event becomes small, and double ionization is instead described by the ''sudden approximation'' where, after ejection of the first electron by the projectile nucleus, the atomic wave function of the target helium changes to the ionic wave function, leaving the second electron still in its original atomic eigenenergy state. This electron can then be ''shaken off,'' since the matrix element between the atomic state (containing the electron-electron interaction) and the asymptotic ionic state (without electron-electron interaction) is nonzero. For the latter process, the ratio $R$ of double-to-single ionization is expected to be constant [2].

## II. EXPERIMENTAL PROCEDURE

This work was done using the tandem Van de Graaff accelerator at Western Michigan University using techniques similar to those used previously [4]. A schematic of the experimental setup is shown in Fig. 1. After passing through two sets of slits, the $Li^{q+}$ ($q$=1,2,3) projectiles were directed into the 4-cm-long collision chamber where they collided with the helium target gas. The pressure in the collision chamber was measured with a capacitance manometer. Outgoing $Li^{0,1,2,3+}$ charge-changed reaction products were separated with a magnet, and subsequently observed with surface-barrier detectors. The incident beam was collected in a Faraday cup. To detect coincidences between the charge-changed Li ions and the ionized target atoms, the recoiling $He^+$ and $He^{2+}$ ions were deflected by a transverse electric field into a detector with a microchannel plate which could be operated to about 25 kHz. To detect coincidences between the unchanged Li ions and the He recoil ions, the unchanged ions were detected with a solid-state detector which required

*Present address: Physics Division, Oak Ridge National Laboratory, Oak Ridge, TN 37831-6372.
†Present address: Dept. of Physics, Kansas State University, Manhattan, KS 66506.

 

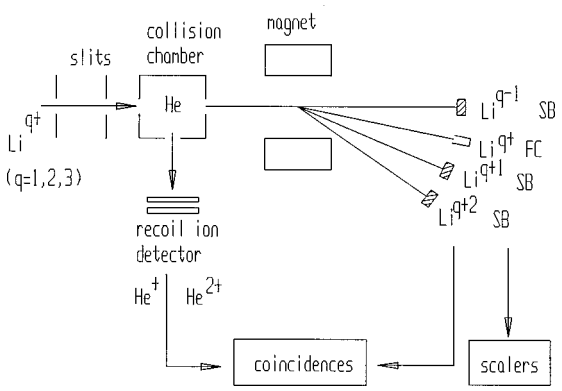


FIG. 1. Schematic of the experimental arrangement. FC is a Faraday cup, SB a surface-barrier detector.

the beam current to be decreased by a factor of about 100. Considerable care was taken to ensure that events were not ''lost'' due to settings of the electronics. Care was also taken to ensure that contaminants in the supply gas did not affect the measured event yields. See Ref. [5] for a more complete discussion of the latter two points.

## III. DATA ANALYSIS AND RESULTS

### A. Singles

The total charge changing, i.e., singles, measurements (without the recoil-ion detector and the coincidence electronics in place) were done for 0.5–8-MeV $Li^{+}$, 3–16-MeV $Li^{2+}$, and 3–20-MeV $Li^{3+}$+He collisions. In the case of single capture, accurate knowledge of the cross sections is needed, as these data provide the basis for the determination of the recoil-ion detector efficiency for the coincidence measurements to be discussed below. For each projectile charge state and energy, data were taken for target gas pressures up to 100 mTorr; for single capture to $Li^{3+}$ at energies above 10 MeV, target gas pressures up to 200 mTorr were used. In these measurements, care was taken to ensure that the total charge-changing fraction of the incident beam did not exceed about 10%, and that single-collision conditions prevailed.

The results for single-electron capture and loss are listed in Table I and shown in Figs. 2(a) and 3(a). Statistical uncertainties for these measurements are due to fitting the fractional yield vs pressure curves (5%), while systematic uncertainties are due to the effective length of the collision chamber (2%), inaccuracy of the pressure reading in the collision region (5%), and the calibration of the measured beam current (4%).

### B. Coincidences

For the coincidence experiment, measurements were carried out for each incident projectile charge state and reaction channel (single capture, single loss, and direct ionization) at impact energies in the range 2–8 MeV for $Li^{+}$, 3–16 MeV for $Li^{2+}$, and 3–20 MeV for $Li^{3+}$. Each of these measurements was done for target gas pressures in the range 0–1 mTorr, where single-collision conditions prevailed. Double-collision contributions to the measured yields from charge exchange prior to entering the target region were in general less than 5% [5]. We note that for these coincidence measurements much lower target gas pressures are required than for the singles measurements, because the relatively slow moving recoiling He ions have a high probability for changing their charge in the target gas as they are accelerated to the recoil-ion detector (Fig. 1).

TABLE I. Cross sections for total single-electron capture ($\sigma_{q,q-1}$) and single-electron loss ($\sigma_{q,q+1}$, in $Li^{1,2,3+}$+He collisions. The number in square brackets represents the power of 10.

| $E$ (MeV) | $\sigma_{q,q-1}$ (cm$^2$) | $\sigma_{q,q+1}$ (cm$^2$) |
|---|---|---|
| | $Li^{+}$ projectile | |
| 0.50 | $(2.0\pm0.4)[-17]$ | $(1.6\pm0.3)[-17]$ |
| 0.75 | $(1.0\pm0.2)[-17]$ | $(2.4\pm0.5)[-17]$ |
| 1.00 | $(5.6\pm1.1)[-18]$ | $(2.4\pm0.5)[-17]$ |
| 1.50 | $(2.2\pm0.4)[-18]$ | $(2.6\pm0.5)[-17]$ |
| 2.00 | $(1.0\pm0.2)[-18]$ | $(2.3\pm0.5)[-17]$ |
| 4.00 | $(1.2\pm0.2)[-19]$ | $(1.8\pm0.4)[-17]$ |
| 6.00 | $(2.4\pm0.5)[-20]$ | $(1.2\pm0.3)[-17]$ |
| 7.00 | $(1.5\pm0.3)[-20]$ | $(1.2\pm0.2)[-17]$ |
| 8.00 | $(8.0\pm1.6)[-21]$ | $(1.0\pm0.2)[-17]$ |
| | $Li^{2+}$ projectile | |
| 3.00 | $(2.3\pm0.3)[-18]$ | $(6.2\pm1.2)[-18]$ |
| 4.50 | $(5.3\pm1.1)[-19]$ | $(5.1\pm1.0)[-18]$ |
| 6.00 | $(1.7\pm0.3)[-19]$ | $(4.2\pm0.8)[-18]$ |
| 8.00 | $(5.2\pm1.0)[-20]$ | $(3.5\pm0.7)[-18]$ |
| 10.0 | $(1.9\pm0.4)[-20]$ | |
| 14.0 | $(3.5\pm0.7)[-21]$ | $(2.9\pm0.6)[-18]$ |
| 16.0 | $(3.0\pm0.6)[-21]$ | $(1.8\pm0.4)[-18]$ |
| | $Li^{3+}$ projectile | |
| 3.00 | $(6.7\pm1.3)[-18]$ | |
| 4.00 | $(2.4\pm0.5)[-18]$ | |
| 6.00 | $(4.9\pm1.0)[-19]$ | |
| 8.00 | $(1.5\pm0.3)[-19]$ | |
| 10.0 | $(5.2\pm1.0)[-20]$ | |
| 12.0 | $(2.2\pm0.4)[-20]$ | |
| 16.0 | $(5.5\pm1.1)[-21]$ | |
| 20.0 | $(2.4\pm0.5)[-21]$ | |

The ratios $R$ of double-to-single target ionization could be determined for each Li projectile reaction (no charge change, single-electron loss, and single-electron capture) directly from the number of detected $He^{+}$ and $He^{2+}$ events without knowledge of the efficiency of the recoil-ion detector. In order to determine absolute coincidence cross sections, however, the efficiency of the recoil-ion detector had to be known. The determination of this efficiency was based on the fact that for single-electron capture in a helium target only single or double ionization of the target can occur, i.e.,

$$\sigma_{q,q-1}=\sigma^{01}_{q,q-1}+\sigma^{02}_{q,q-1}=\sigma^{01}_{q,q-1}(1+\sigma^{02}_{q,q-1}/\sigma^{01}_{q,q-1})$$
$$=\sigma^{01}_{q,q-1}(1+R_{q,q-1}), \quad (1)$$

where $\sigma_{q,q-1}$, $\sigma^{01}_{q,q-1}$, and $\sigma^{02}_{q,q-1}$ are the cross sections for total single capture, and single capture associated with single and double ionization of the target, respectively, and $R_{q,q-1}$ is the ratio of target double-to-single ionization associated with single-electron capture to the projectile. From the mea-

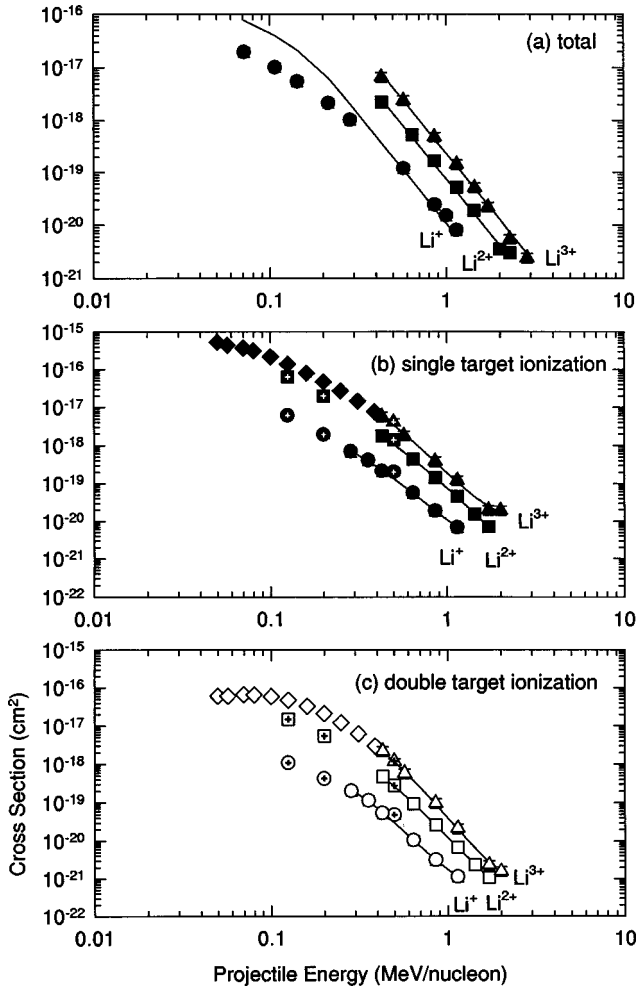


FIG. 2. (a) Cross sections for total single-electron capture by the projectile in $Li^{1,2,3+}$+He collisions. All data are from this work. The solid lines are the empirical predictions from Ref. [6]. (b) and (c) Cross sections for single (solid symbols) and double (open symbols) ionization of He by $Li^{1,2,3+}$ projectiles undergoing single-electron capture. Symbols are as follows: (●, ○)—$Li^{+}$, this work; (⊕, ⊕)—$Li^{+}$, Ref. [10]; (■,□)—$Li^{2+}$, this work; (⊞,⊞)—$Li^{2+}$, Ref. [10]; (▲,△)—$Li^{3+}$, this work; (▲,⧋)—$Li^{3+}$, Ref. [10]; (◆,◇)—$Li^{3+}$, Ref. [9]. The lines are drawn to guide the eye through the present data.

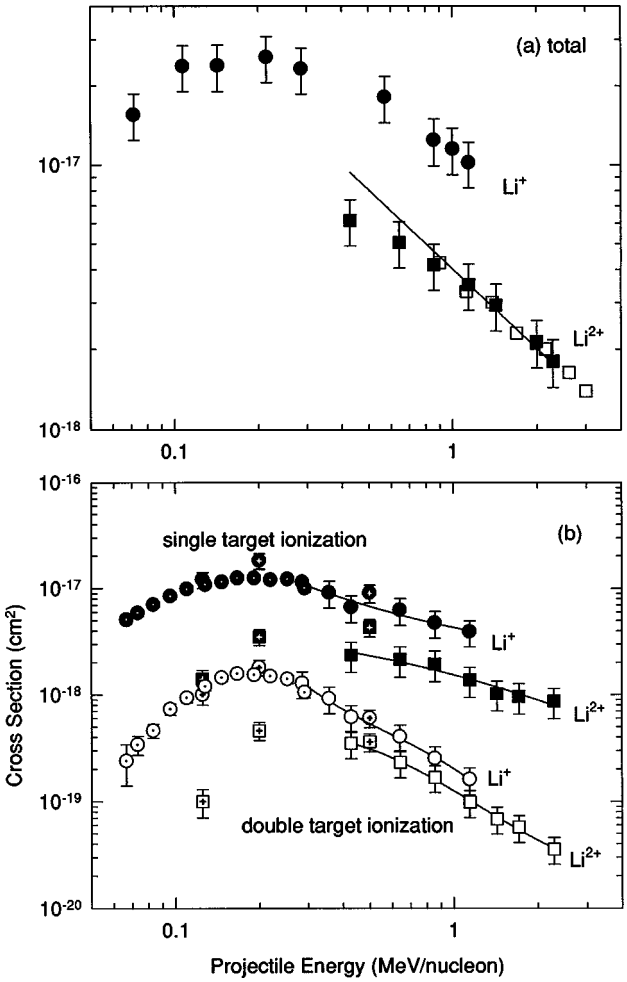


FIG. 3. (a) Cross sections for total single-electron loss from the projectile in $Li^{1,2+}$+He collisions. Solid symbols are data from this work and the open symbols (for $Li^{2+}$) are from Ref. [7]. The solid line shows the prediction of the Bohr model [8] for $Li^{2+}$. (b) Cross sections for single (solid symbols) and double (open symbols) ionization of He by $Li^{1,2+}$ projectiles undergoing single-electron loss. Symbols are as follows: (●,○)—$Li^{+}$, this work; (⊕, ⊕)—$Li^{+}$, Ref. [10]; (●, ⊙)—$Li^{+}$, Ref. [11]; (■,□)—$Li^{2+}$, this work; (⊞,⊞)—$Li^{2+}$, Ref. [10]. The lines are drawn to guide the eye through the present data.

sured ratios $R_{q,q-1}$ (Table II) and the measured total single-capture cross sections for $Li^{1,2,3+}$ (Table I), the efficiency $\epsilon$ of the recoil-ion detector was determined from

$$\sigma_{q,q-1} = Y^{01}_{q,q-1}(1+R_{q,q-1})\epsilon, \tag{2}$$

where $Y^{01}_{q,q-1}$ is the measured yield for single ionization of the target associated with single capture. The resulting efficiency of the recoil-ion detector was found to be about $\epsilon = 0.5 \pm 0.1$, and this value was used to calculate the coincidence cross sections for direct target ionization (no projectile charge change) and for target ionization associated with projectile loss. For target ionization associated with single capture by the projectile, the cross sections can be calculated directly from Eq. (1). Thus, by comparing the values of these latter cross sections with the same cross sections obtained using the efficiency $\epsilon$, an independent check of the efficiency is obtained.

The determined cross sections, and the cross-section ratios, for single and double ionization of the helium target associated with single-electron capture, single-electron loss, and no charge change, are listed in Tables II–IV and are shown in Figs. 2(b), 2(c), 3(b), and 4, respectively. The uncertainties for the singles experiment listed above also apply to the coincidence measurements. In addition, there are the reproducibility error (15%) and the uncertainty of the recoil-ion detector efficiency (20%), thus giving an overall uncertainty of about 30% in the listed cross-section values.

## IV. DISCUSSION

### A. Cross sections

For the single cross sections, Fig. 2(a) shows that the single-capture cross sections for $Li^{1,2,3+}$+He decrease with

TABLE II. Cross sections for single ($\sigma^{01}_{q,q-1}$) and double ($\sigma^{02}_{q,q-1}$) ionization and ratios ($R_{q,q-1}$) of double-to-single ionization of He by $Li^{1,2,3+}$ projectiles undergoing single-electron capture. The cross sections for double ionization were determined from $\sigma^{02}_{q,q-1}=\sigma^{01}_{q,q-1}R_{q,q-1}$.

| $E$ (MeV) | $\sigma^{01}_{q,q-1}$ (cm$^2$) | $\sigma^{02}_{q,q-1}$ (cm$^2$) | $R_{q,q-1}$ (%) |
|---|---|---|---|
| | $Li^+$ projectile | | |
| 2.00 | (6.9±1.9)[−19] | (2.0±0.6)[−19] | 29.5±0.3 |
| 2.50 | (4.1±1.2)[−19] | (1.1±0.3)[−19] | 27.9±0.5 |
| 3.00 | (2.1±0.6)[−19] | (5.3±1.5)[−20] | 25.1±0.9 |
| 4.50 | (5.6±1.6)[−20] | (1.1±0.3)[−20] | 18.9±1.5 |
| 6.00 | (1.9±0.5)[−20] | (3.2±0.9)[−21] | 16.9±0.8 |
| 8.00 | (6.9±1.9)[−21] | (1.1±0.3)[−21] | 16.6±2.8 |
| | $Li^{2+}$ projectile | | |
| 3.00 | (1.8±0.5)[−18] | (4.8±1.3)[−19] | 26.9±1.0 |
| 4.50 | (4.3±1.2)[−19] | (9.3±2.6)[−20] | 21.5±0.5 |
| 6.00 | (1.4±0.4)[−19] | (2.6±0.8)[−20] | 18.8±1.6 |
| 8.00 | (4.5±1.3)[−20] | (6.8±1.9)[−21] | 15.1±0.6 |
| 10.0 | (1.5±0.4)[−20] | (2.2±0.6)[−21] | 14.9±1.5 |
| 12.0 | (7.1±2.0)[−21] | (1.1±0.3)[−21] | 14.9±0.1 |
| | $Li^{3+}$ projectile | | |
| 3.00 | (5.8±1.6)[−18] | (2.2±0.6)[−18] | 37.8±1.7 |
| 4.00 | (1.8±0.5)[−18] | (5.8±1.6)[−19] | 32.0±1.9 |
| 6.00 | (3.9±1.1)[−19] | (10.0±2.8)[−20] | 25.5±0.9 |
| 8.00 | (1.2±0.3)[−19] | (2.1±0.5)[−20] | 17.7±0.1 |
| 12.0 | (2.0±0.6)[−20] | (2.4±0.8)[−21] | 11.8±1.2 |
| 14.0 | (2.0±0.6)[−20] | (1.6±0.5)[−21] | 8.1±0.7 |

increasing energy and decreasing incident charge state, as expected. In the energy regime represented by the present work, the data are well represented by the empirical scaling rule of Schlachter *et al.* [6], except for $Li^+$ at the lowest measured energies. A similar deviation from this scaling rule at low energies was observed in the work of Ref. [4] for $He^+$+He collisions (also $q=1$). For single-electron loss from the projectile, shown in Fig. 3(a), the cross sections for $Li^+$ are seen to be significantly larger than those for $Li^{2+}$, as expected. However, this effect is enhanced due to the fact that the incident $Li^+$ beam contained a significant metastable fraction determined to be about 20% [5]. The present data for $Li^{2+}$ are seen to be in very good agreement with earlier results of Hülskötter *et al.* [7]. Furthermore, at the highest energies investigated, the data for $Li^{2+}$ are in good agreement with predictions of the Bohr model, as formulated by Knudsen *et al.* [8].

TABLE III. Cross sections for single ($\sigma^{01}_{q,q+1}$) and double ($\sigma^{02}_{q,q+1}$) ionization and ratios ($R_{q,q+1}$) for double-to-single ionization of He by $Li^{1,2+}$ projectiles undergoing single-electron loss. The cross sections for double ionization were determined from $\sigma^{02}_{q,q+1}=\sigma^{01}_{q,q+1}\times R_{q,q+1}$.

| $E$ (MeV) | $\sigma^{01}_{q,q+1}$ (cm$^2$) | $\sigma^{02}_{q,q+1}$ (cm$^2$) | $R_{q,q+1}$ (%) |
|---|---|---|---|
| | $Li^+$ projectile | | |
| 2.00 | (1.1±0.3)[−17] | (1.2±0.3)[−18] | 11.2±0.3 |
| 2.50 | (9.1±2.6)[−18] | (9.2±2.6)[−19] | 10.1±0.3 |
| 3.00 | (6.6±1.9)[−18] | (6.1±1.7)[−19] | 9.3±0.6 |
| 4.50 | (6.3±1.8)[−18] | (4.1±1.2)[−19] | 6.5±0.3 |
| 6.00 | (4.7±1.3)[−18] | (2.5±0.7)[−19] | 5.3±0.2 |
| 8.00 | (3.9±1.1)[−18] | (1.6±0.5)[−19] | 4.1±0.2 |
| | $Li^{2+}$ projectile | | |
| 3.00 | (2.4±0.7)[−18] | (3.6±1.2)[−19] | 14.8±2.4 |
| 4.50 | (2.1±0.7)[−18] | (2.3±0.7)[−19] | 10.8±1.8 |
| 6.00 | (1.9±0.6)[−18] | (1.7±0.5)[−19] | 8.7±1.5 |
| 8.00 | (1.4±0.4)[−18] | (10.1±3.3)[−20] | 7.2±1.2 |
| 10.0 | (1.0±0.3)[−18] | (6.8±2.4)[−20] | 6.8±1.3 |
| 12.0 | (9.6±3.1)[−19] | (5.8±2.3)[−20] | 6.0±1.3 |
| 16.0 | (8.7±2.8)[−19] | (3.6±1.0)[−20] | 4.1±0.8 |

TABLE IV. Cross sections for single ($\sigma^{01}_{q,q}$) and double ($\sigma^{02}_{q,q}$) ionization and ratios ($R_{q,q}$) of double-to-single ionization of He by $Li^{1,2,3+}$ projectiles undergoing no charge change. The cross sections for double ionization were determined from $\sigma^{02}_{q,q}=\sigma^{01}_{q,q}\times R_{q,q}$.

| $E$ (MeV) | $\sigma^{01}_{q,q}$ (cm$^2$) | $\sigma^{02}_{q,q}$ (cm$^2$) | $R_{q,q}$ (%) |
|---|---|---|---|
| | $Li^+$ projectile | | |
| 2.00 | (9.8±2.7)[−17] | (4.8±1.4)[−18] | 4.9±0.1 |
| 2.50 | (8.4±2.3)[−17] | (3.6±1.0)[−18] | 4.3±0.1 |
| 3.00 | (7.1±2.0)[−17] | (2.7±0.8)[−18] | 3.8±0.1 |
| 4.50 | (5.2±1.5)[−17] | (1.4±0.4)[−18] | 2.7±0.1 |
| 6.00 | (4.0±1.1)[−17] | (8.8±2.5)[−19] | 2.2±0.3 |
| 8.00 | (3.7±1.0)[−17] | (6.0±1.7)[−19] | 1.6±0.1 |
| | $Li^{2+}$ projectile | | |
| 3.00 | (1.9±0.5)[−16] | (6.7±1.9)[−18] | 3.5±0.3 |
| 4.50 | (1.2±0.3)[−16] | (2.9±0.7)[−18] | 2.4±0.1 |
| 6.00 | (9.1±2.6)[−17] | (1.7±0.5)[−18] | 1.9±0.1 |
| 8.00 | (8.2±2.3)[−17] | (1.2±0.3)[−18] | 1.5±0.1 |
| 10.0 | (5.8±1.6)[−17] | (7.0±2.0)[−19] | 1.2±0.1 |
| 12.0 | (5.9±1.7)[−17] | (5.3±1.6)[−19] | 0.9±0.1 |
| 16.0 | (4.5±1.3)[−17] | (3.6±1.4)[−19] | 0.8±0.2 |
| | $Li^{3+}$ projectile | | |
| 3.00 | (3.3±0.1)[−16] | (1.5±0.1)[−17] | 4.5±0.1 |
| 4.00 | (2.4±0.7)[−16] | (8.4±2.4)[−18] | 3.5 ± 0.2 |
| 6.00 | (1.7±0.5)[−16] | (4.1±1.2)[−18] | 2.4±0.0 |
| 12.0 | (1.2±0.3)[−16] | (1.4±0.4)[−18] | 1.2±0.0 |
| 16.0 | (8.4±2.3)[−17] | (8.4±2.3)[−19] | 1.0±0.1 |
| 20.0 | (7.5±2.1)[−17] | (6.0±1.8)[−19] | 0.8±0.1 |
| 24.0 | (6.4±1.8)[−17] | (4.5±1.3)[−19] | 0.7±0.0 |

Considering the coincidence cross sections, for the direct ionization channel shown in Fig. 4, the present results are consistent with earlier results of other investigators [3,9,10], except those for $Li^+$ associated with single and double target ionization measured by Knudsen *et al.* [3]. It is not clear why this is so but it could be due to a different fraction of metastable ions in the incident $Li^+$ beam. For the single capture channel [Figs. 2(b) and 2(c)], the present experiment provides data in the energy regime above 400 keV/nucleon for all three Li charge states. In the region of overlap with other measurements at lower energies, there is good agreement with the data of Shah and Gilbody [9] and Sanders [10]. For the single-loss channel [Fig. 3(b)] in the region of overlap, the present data for $Li^+$ agree well with the data of Ref. [11]. Also, the double target ionization data of Ref. [10] agree

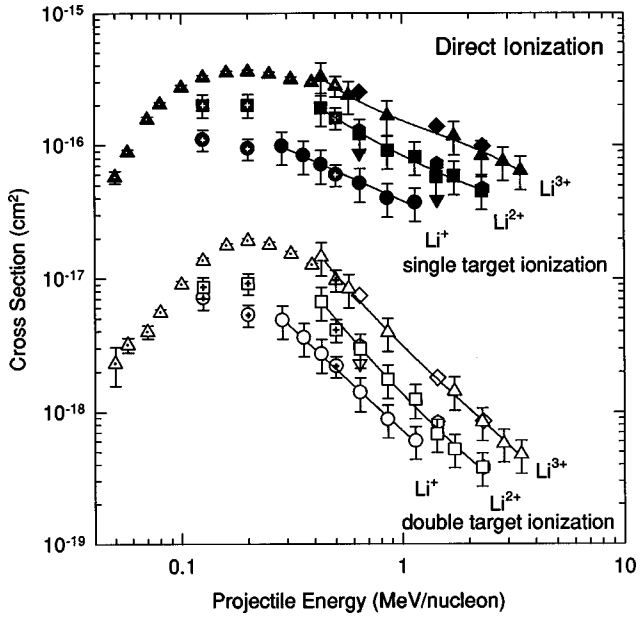


FIG. 4. Cross sections for single (solid symbols) and double (open symbols) ionization of He by $Li^{1,2,3+}$ projectiles undergoing no charge change (direct ionization). Symbols are as follows: (●,○)—$Li^+$, this work; (◖,⊕)—$Li^+$, Ref. [10]; (▼,▽)—$Li^+$, Ref. [3]; (■,□)—$Li^{2+}$, this work; (◧,⊞)—$Li^{2+}$, Ref. [10]; (◖,○)—$Li^{2+}$, Ref. [3]; (▲,△)—$Li^{3+}$, this work; (◭,⊞)—$Li^{3+}$, Ref. [10]; (◆,◇)—$Li^{3+}$, Ref. [3]; (◭,△)—$Li^{3+}$, Ref. [9]. The lines are drawn to guide the eye through the present data.

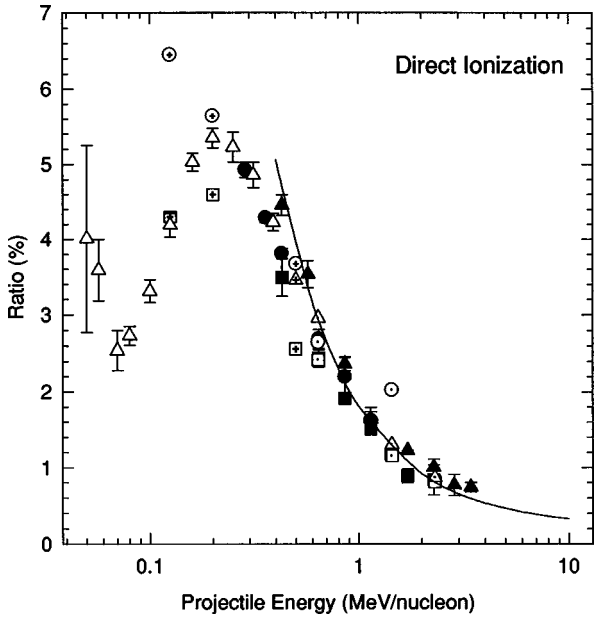


FIG. 5. He target double-to-single ionization ratios associated with direct ionization (no charge change) for $Li^{1,2,3+}$ projectiles. Symbols are as follows: (●)—$Li^+$, this work; (⊕)—$Li^+$, Ref. [10]; (⊙)—$Li^+$, Ref. [3]; (■)—$Li^{2+}$, this work; (⊞)—$Li^{2+}$, Ref. [10]; (⊡)—$Li^{2+}$, Ref. [3]; (▲)—$Li^{2+}$, this work; (◭)—$Li^{3+}$, Ref. [10]; (△)—$Li^{3+}$, Ref. [3]; (△)—$Li^{3+}$, Ref. [9]. The smooth curve is the scaling rule of Ref. [1] for $Li^{3+}$+He.

well, while the single target ionization data of Ref. [10] are higher than the present data. From Figs. 2–4 it is seen that for all collision reactions (single-electron capture, single-electron loss, and no charge change), and for all incoming projectile charges ($Li^{1,2,3+}$), the cross sections for double target ionization are one to two orders of magnitude smaller than the cross sections for single target ionization. This result is consistent with the expectation that double target ionization requires a ''harder'' collision, i.e., the average impact parameter for the collision is smaller.

A good measure of the collective influence of the projectile electrons on the collision process is the effective charge. In this case, the projectile electrons are considered as an electron cloud which ''screens'' the nuclear charge. In the present energy regime (0.5–8 MeV/$q$), the two-step mechanism [3,12,13] for double ionization is expected to be dominant, i.e., the projectile interacts strongly with the two target electrons in separate encounters. In this case, single and double ionization are expected to scale like $(q_{\rm eff}/v)^2$ and $(q_{\rm eff}/v)^4$, respectively, where $q_{\rm eff}$ is the effective charge of the projectile as seen by the target. Thus, these relations can be used to calculate the effective charges of $Li^+$ and $Li^{2+}$ for target ionization by normalizing the direct ionization cross sections for these projectiles to those of the bare projectile $Li^{3+}$. For $Li^+$, the average effective charges for single and double ionization are found to be 1.4 and 2.0, respectively, while the average effective charges for single and double ionization by $Li^{2+}$ are 2.1 and 2.4, respectively.

McGuire, Stolterfoht, and Simony [14] proposed a theory for the effective charge of a hydrogenic projectile based on the *screening* and *antiscreening* mechanisms. At distant collisions such a projectile with nuclear charge $Z$ is fully screened, so that

$$|q_{\rm eff}^{\rm distant}|^2=|Z-1|^2, \tag{3}$$

while at close collisions the projectile nucleus and the projectile electrons collide independently with the target, so that the effective charge is larger than the nuclear charge:

$$|q_{\rm eff}^{\rm close}|^2=Z^2+1. \tag{4}$$

For the hydrogenic projectile $Li^{2+}$, Eqs. (3) and (4) predict an effective charge of 2.0 for distant collisions, and 3.2 for close collisions. The experimentally determined effective charge for single ionization ($q_{\rm eff}$=2.1) is close to the distant-collision limit, while the effective charge for double ionization ($q_{\rm eff}$=2.4) is somewhere between the close encounter and the distant-encounter limits. These results show quantitatively that collisions producing double ionization require a smaller impact parameter than collisions producing single ionization, as expected, and are consistent with results of Forest *et al.* [4] for $He^+$+He collisions.

### B. Ratios of double-to-single ionization

Of primary interest in this work is the ratio of double-to-single ionization of the He target, because this ratio can be used to exhibit the main features of double ionization [1–3,12,13]. Here these ratios are investigated experimentally as a function of the incoming projectile charge state and as a function of the outgoing reaction channel, as shown in Figs. 5–7. From these plots, three observations are made: (1) For a given incident projectile charge state, the ratios depend

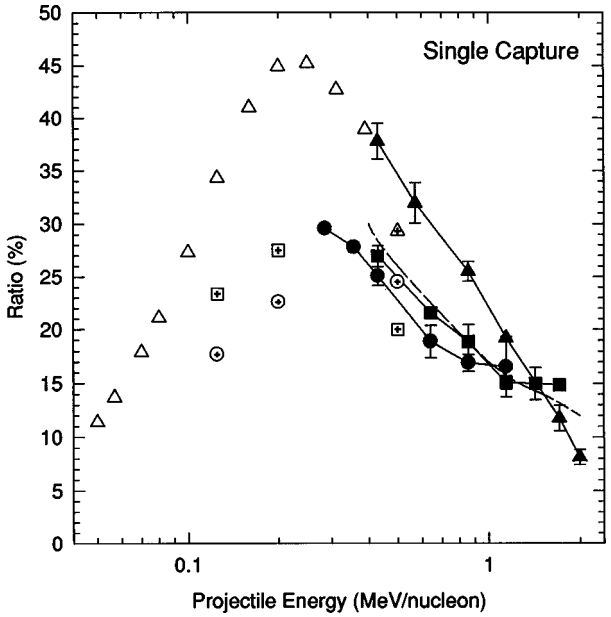


FIG. 6. He target double-to-single ionization ratios associated with single-electron capture for $Li^{1,2,3+}$ projectiles. Symbols are as follows: (●)—$Li^{+}$, this work; (⊕)—$Li^{+}$, Ref. [10]; (■)—$Li^{2+}$, this work; (⊞)—$Li^{2+}$, Ref. [10]; (▲)—$Li^{3+}$, this work; (⧋)—$Li^{3+}$, Ref. [10]; (△)—$Li^{3+}$, Ref. [9]. The solid lines are drawn to guide the eye. The dashed curve shows the calculated values from Ref. [15] for $Li^{3+}$.

strongly on the outgoing reaction channel, specifically, $R_{q,q-1}>R_{q,q+1}>R_{q,q}$; (2) For direct ionization (no charge change) at a given energy, the ratios are largely independent of the incoming projectile charge state (Fig. 5), depending essentially only on the nuclear charge; and (3) for single-electron capture and single-electron loss, the ratios depend quite strongly on the incoming projectile charge state (Figs. 6 and 7).

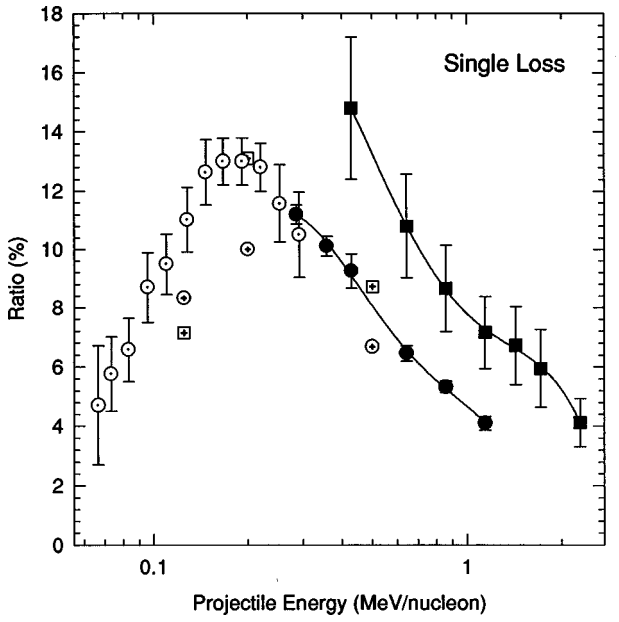


FIG. 7. He target double-to-single ionization ratios associated with single-electron loss for $Li^{1,2+}$ projectiles. Symbols are as follows: (●)—$Li^{+}$, this work; (⊕)—$Li^{+}$, Ref. [10]; (⊙)—$Li^{+}$, Ref. [11]; (■)—$Li^{2+}$, this work; (⊞)—$Li^{2+}$, Ref. [10]. The lines are drawn to guide the eye.

Observation (1) can be understood qualitatively in terms of the average impact parameters for the three types of collision reactions. The larger the ratio, the more double ionization which takes place compared to single ionization. Double ionization is generally expected to require smaller impact parameter collisions than single ionization, as evidenced by the higher effective charge $q_{\rm eff}$ found for double ionization in the above discussion. Therefore, the average impact parameter for the single capture reaction channel appears to be smaller than for the single-loss channel, which, in turn, is smaller than the average impact parameter for direct ionization.

#### *1. Direct target ionization*

According to observation (2), the ratio $R_{q,q}$ for direct ionization is nearly independent of the number of electrons on the impacting projectile. Figure 5 shows that for energies $\gtrsim 0.3$ MeV/nucleon the measured ratios for incident $Li^{1,2,3+}$ are all nearly the same, and fall along the predicted scaling rule of Knudsen *et al.* [3] for $Li^{3+}$. A similar result was previously obtained by Forest *et al.* [4], who reported that the double-to-single ionization ratios at a given energy for $He^{+}+He$ and $He^{2+}+He$ collisions are nearly the same in this velocity regime.

For fully stripped projectiles of nuclear charge $Z$ and velocities $v$ such that $Z/v \lesssim 1$ ($v$ in atomic units), the ratio $R$ of double-to-single ionization is given by [2,3,12,13]

$$R=C_1+C_{\rm int}\left(\frac{Z}{v}\right)+C_2\left(\frac{Z}{v}\right)^2, \tag{5}$$

where the first term is due to the one-step mechanism (ionization involving electron-electron interactions), the last term results from the two-step mechanism (independent-particle ionization), and the middle term comes from interference between the one- and two-step mechanisms. The validity of this scaling for fully stripped projectiles at intermediate-to-high velocities has been well established [12].

On the contrary, little is known about the behavior of $R$ for projectiles which are not fully stripped. In general, it is expected that

$$R=R(q,Z,v). \tag{6}$$

From Fig. 5 for direct ionization, however, it is apparent that for $Li^{1,2,3+}$ projectiles in the energy range investigated here there is little dependence of $R$ on $q$, i.e., $R \neq R(q)$, and so $R$ is given essentially by Eq. (5). Since this equation, and consequently the empirical scaling rule of Knudsen *et al.* [3], were derived only for *bare* projectiles impacting on He, it is not clear *a priori* that these should be valid for partially stripped projectiles as well.

The results of Fig. 5 suggest that the electrons on the projectile have little influence on the *ratio* of double-to-single ionization. However, the absolute single and double ionization *cross sections* at a given energy do decrease with decreasing projectile charge state, as seen in Fig. 4. Thus, it must be concluded that whatever effect the projectile elec-

trons have on the single ionization cross sections compared to $Li^{3+}$, they have nearly the same effect on the double ionization cross sections.

### 2. Target ionization with projectile capture or loss

Contrary to the results for direct ionization, the ratios $R_{q,q-1}$ and $R_{q,q+1}$ for target ionization accompanied by projectile single capture or loss, respectively, depend quite strongly on the incident projectile charge state, as seen in Figs. 6 and 7. In the single-capture channel (Fig. 6) the ratios for $Li^+$ and $Li^{2+}$ exhibit approximately the same behavior, have nearly the same magnitude, and appear to level off at the highest energies investigated. The ratios for $Li^{3+}$, however, are still decreasing for the highest energies investigated. In the range 0.3 to about 1.5 MeV/nucleon, the ratios for $Li^{3+}$ are larger than those for $Li^+$ and $Li^{2+}$, while for energies $\gtrsim$1.5 MeV/nucleon the ratios for $Li^{3+}$ are smaller. These results suggest the importance of the electron-electron interaction in this reaction channel. At the lower velocities the bare projectile produces relatively more double ionization (due to the electron-nucleus interaction) than the nonbare projectiles (due to a combination of electron-nucleus and electron-electron interactions), while at the highest velocities investigated here the situation is reversed. Thus, the strength of the electron-electron interaction apparently increases compared to the electron-nucleus interaction as the collision velocity increases.

Knudsen *et al.* [15] and McGuire, Salzborn, and Müller [16] analyzed data for target ionization accompanied by single capture (which they refer to as simultaneous capture and ionization) in terms of direct (two-step) and rearrangement (one-step) mechanisms. The direct contribution is calculated assuming independent capture and ionization probabilities [16], while the rearrangement contribution was calculated from second Born terms [15]. In Fig. 6 we show the calculated curve for $Li^{3+}$+He from Ref. [15]. It is seen that this curve underestimates the present data for energies $\lesssim$1.5 MeV/nucleon. Above this energy, the calculated curve levels off somewhat while the $Li^{3+}$ data continue to decrease strongly. Noteworthy is the fact that the calculated curve agrees quite well with the $Li^{2+}$ ratios, and to a lesser degree with the $Li^+$ ratios. While this latter agreement may be fortuitous, it is clear that more work needs to be done to understand the scaling of the double-to-single ionization ratios in the single-capture channel.

In the single-loss channel (Fig. 7), the ratios $R_{q,q+1}$ for $Li^+$ and $Li^{2+}$ exhibit a behavior similar to each other, with the $Li^{2+}$ ratios being approximately 80% larger than the $Li^+$ results. Thus $Li^{2+}$ causes more target double ionization for a given amount of target single ionization than $Li^+$. This is evidence that the electronic structure of the projectile plays an important role in this reaction.

It has been suggested that such results can be interpreted in the free-collision model [8,17]. In this model, collision processes such as $Li^{2+}$+He and $He^+$+He reduce to collisions of He targets with bare projectiles, namely, $Li^{3+}$ and $He^{2+}$, respectively, where the projectiles do not change charge state, plus the scattering of a free electron accompanying these processes, i.e., $e^-$+He. Electrons in the collision reaction have a dual role: they can (a) shield the nucleus

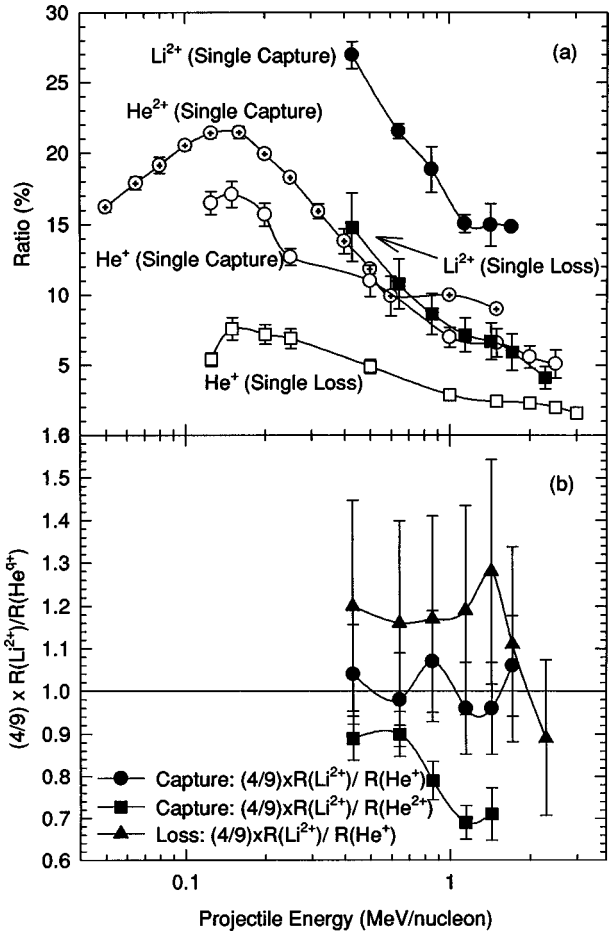


FIG. 8. (a) He target double-to-single ionization ratios associated with single-electron capture and loss for $Li^{2+}$, $He^{2+}$, and $He^+$ projectiles. Symbols are as follows: Single capture: (●)—$Li^{2+}$, this work; (⊕)—$He^{2+}$, (○)—$He^+$, Refs. [1,4,13]. Single loss: (■)—$Li^{2+}$, this work, (□)—$He^+$, Ref. [4]. (b) Ratios $\frac{4}{9}R(Li^{2+})/R(He^{q+})$ for double-to-single ionization ratios associated with single capture to hydrogenic projectiles (●) and to projectiles of ionic charge 2 (■), and for double-to-single ionization ratios associated with single loss from hydrogenic projectiles (▲). The lines are drawn to guide the eye.

(screening) or (b) ionize the electron(s) of the collision partner (antiscreening).

In the screening process (direct ionization), the electrons remain in their original state, while in the antiscreening process they actively participate in the collision and can be ionized or excited [14,18,19]. Screening is characterized by an electron-nucleus interaction, while antiscreening involves an electron-electron interaction. Screening and the projectile excitation contribution of antiscreening both leave the projectile in the same charge state [18], so that they cannot be distinguished in this experiment. Thus antiscreening associated with projectile excitation is included in the direct ionization channel here. However, for double ionization of the helium target, it can be concluded that the ionization part of antiscreening (single loss reaction channel) is relatively more important than screening and the excitation part of antiscreening combined (direct ionization). This can be seen from Figs. 5 and 7, where the ratios for single loss from $Li^+$ and $Li^{2+}$ are significantly larger than the ratios for direct

ionization by the same ions at all energies investigated.

To give additional insight into the effect of the projectile electrons on the double-to-single ionization ratio for the single capture and loss reaction channels, the results for the hydrogenic projectile $Li^{2+}$ can be compared with $He^{+}$ (which has the same electronic structure) and with $He^{2+}$ (which has the same ionic charge). These results are shown in Fig. 8(a). The ratios for capture by $Li^{2+}$ are seen to be about twice as large as those for capture by $He^{2+}$ and capture by $He^{+}$ for energies $>0.4$ MeV/nucleon. The fact that $R_{q,q-1}$ for $Li^{2+}$ is larger than $R_{q,q-1}$ for $He^{2+}$ indicates that it is not simply the ionic charge which is important in this reaction channel. Furthermore, the fact that $R_{q,q-1}$ for $Li^{2+}$ is larger than $R_{q,q-1}$ for $He^{+}$ must be principally due to the higher nuclear charge of $Li^{2+}$, since both $Li^{2+}$ and $He^{+}$ have the same electronic structure, and since the projectile electron is expected to play mainly a passive role in the capture process, i.e., it is a spectator electron. The same cannot be said for the loss channel, i.e., $R_{q,q+1}$ for $Li^{2+}$ and $He^{+}$, where the projectile electron plays an active role in the collision process since it is lost from the projectile. Since the data for energies $\gtrsim 0.4$ MeV/nucleon are in the intermediate-velocity regime, the effect of the nuclear charge on $R$ can be ''taken out'' by considering the ratios $\frac{4}{9}R(Li^{2+})/R(He^{q+})$, with $q=1,2$. These results are shown in Fig. 8(b). It is seen that these ratios for capture to isoelectronic $Li^{2+}$ and $He^{+}$ are nearly unity, indicating that whatever effect the projectile electron has on $R_{q,q-1}$ it is the same for $Li^{2+}$ and $He^{+}$. Thus, the net effect of the $Li^{2+}$ electron on $R_{q,q-1}$ should be shown by the ratios $\frac{4}{9}R(Li^{2+})/R(He^{2+})$ for capture to $Li^{2+}$ and $He^{2+}$. These latter ratios are less than unity, and appear to generally decrease with increasing projectile velocity, indicating that the $Li^{2+}$ (spectator) electron serves to decrease the relative amount of double ionization, perhaps due to screening. Finally, it is seen that the ratios $\frac{4}{9}R(Li^{2+})/R(He^{+})$ for loss from $Li^{2+}$ and $He^{+}$ are generally greater than unity and appear to decrease for energies $\gtrsim 1$ MeV/nucleon. This result for $R_{q,q+1}$ indicates that the projectile electron produces greater double ionization as the nuclear charge increases, perhaps signaling the increasing importance of electron-electron (anti-screening) effects for higher-$Z$ projectiles. The theoretical basis for these observations is not known.

## V. CONCLUSIONS

Projectile charge changing and target ionization have been studied for $Li^{q+}$ $(q=1,2,3)$ projectiles colliding with He targets in the energy range between 0.5 and 8 MeV/$q$. Cross sections for single and double ionization of the He target by incident $Li^{1,2,3+}$ have been obtained for three projectile reaction channels, namely, direct ionization, single-electron capture, and single-electron loss. In general, good agreement is found in those cases where previous measurements were available for comparison. For all incoming projectile charge states, energies, and outgoing reaction channels the double ionization cross sections are one to two orders of magnitude smaller than the corresponding single ionization cross sections. This implies that double ionization occurs for smaller average impact parameters than single ionization, as evidenced by the larger calculated effective charges for $Li^{1,2+}$ projectiles for double ionization than for single ionization.

The main emphasis of this work was the investigation of the ratio $R$ of double-to-single ionization of helium for each of the various outgoing reaction channels. It was found that for direct ionization (no charge change) these ratios are largely independent of the incoming projectile charge state and are in good agreement with the scaling of Knudsen *et al.* [3]. Theoretically, however, it is not clear why these ratios are largely independent of the incoming projectile charge state. For the single-capture and the single-loss channels, the ratios depend quite strongly on the incoming projectile charge state, and the contribution of the electron-electron interaction appears to increase compared to the contribution of the electron-nucleus interaction at the highest energies investigated. This is in agreement with studies by Montenegro and co-workers [18,19] for single-electron loss in $He^{+}+(He,H_2)$ collisions.

Finally, while the scaling of the double-to-single ionization ratio for bare projectiles with nuclear charge $Z$ and velocity $v$ is largely understood in the direct ionization channel, the results presented here show that this scaling is not well understood for dressed projectiles or for projectiles undergoing charge change (single-electron capture or single-electron loss). Future experiments for projectiles with $Z>3$ would be useful to enhance the understanding of the $Z$ and $v$ scaling of the ratio for dressed projectiles or for projectiles undergoing single-electron capture or single-electron loss.

## ACKNOWLEDGMENTS

This work was supported in part by the Division of Chemical Sciences, Office of Basic Energy Sciences, Office of Energy Research, U.S. Department of Energy.

[1] J. H. McGuire, Phys. Rev. A **36**, 1114 (1987).
[2] J. H. McGuire, Phys. Rev. Lett. **49**, 1153 (1982).
[3] H. Knudsen, L. H. Andersen, P. Hvelplund, G. Astner, H. Cederquist, H. Danared, L. Liljeby, and K.-G. Rensfelt, J. Phys. B **17**, 3545 (1984).
[4] J. L. Forest, J. A. Tanis, S. M. Ferguson, R. R. Haar, and K. Lifrieri, Phys. Rev. A **52**, 350 (1995).
[5] O. Woitke, Ph.D. thesis, Western Michigan University, 1996 (unpublished).
[6] A. S. Schlachter, J. W. Stearns, K. H. Berkner, M. P. Stockli, W. G. Graham, E. M. Bernstein, M. W. Clark, and J. A. Tanis, in *Fifteenth International Conference on the Physics of Electronic and Atomic Collisions, Brighton, United Kingdom, 1987, Abstracts of Contributed Papers*, edited by J. Geddes, H. B. Gilbody, A. E. Kingston, C. J. Latimer, and H. J. R. Walters (Queen's University Press, Belfast, 1987), p. 505.
[7] H.-P. Hülskötter, B. Feinberg, W. E. Meyerhof, A. Belkacem, J. R. Alonso, L. Blumenfeld, E. A. Dillard, H. Gould, N.

Guardala, G. F. Krebs, M. A. McMahan, M. E. Rhoades-Brown, B. S. Rude, J. Schweppe, S. W. Spooner, K. Street, P. Thieberger, and H. E. Wegner, Phys. Rev. A **44**, 1712 (1991).
[8] H. Knudsen, L. H. Andersen, H. K. Haugen, and P. Hvelplund, Phys. Scr. **26**, 132 (1982).
[9] M. B. Shah and H. B. Gilbody, J. Phys. B **18**, 899 (1985).
[10] J. Sanders (private communication).
[11] M. B. Shah (private communication).
[12] J. H. McGuire, N. Berrah, R. J. Bartlett, J. A. R. Samson, J. A. Tanis, C. L. Cocke, and A. S. Schlachter, J. Phys. B **28**, 913 (1995).
[13] L. H. Andersen, P. Hvelplund, H. Knudsen, S. P. Møller, A. H. Sørensen, K. Elsener, K.-G. Rensfelt, and E. Uggerhøj, Phys. Rev. A **36**, 3612 (1987).
[14] J. H. McGuire, N. Stolterfoht, and P. R. Simony, Phys. Rev. A **24**, 97 (1981).
[15] H. Knudsen, L. H. Andersen, P. Hvelplund, J. Sørensen, and D. Ćirić, J. Phys. B **20**, L253 (1987).
[16] J. H. McGuire, E. Salzborn, and A. Müller, Phys. Rev. A **35**, 3265 (1987).
[17] P. Hvelplund, H. K. Haugen, and H. Knudsen, Phys. Rev. A **22**, 1930 (1980).
[18] E. C. Montenegro, W. E. Meyerhof, and J. H. McGuire, Adv. At., Mol., Opt. Phys. **34**, 249 (1994).
[19] E. C. Montenegro, W. S. Melo, W. E. Meyerhof, and A. G. Pinho, Phys. Rev. Lett. **69**, 3033 (1992).